FIRE AND MATERIALS
Fire Mater. 2007; **31**:297–310
Published online 14 December 2006 in Wiley InterScience (www.interscience.wiley.com). DOI: 10.1002/fam.939

Performance of a non-load-bearing steel stud gypsum board wall assembly: Experiments and modelling‡

Samuel L. Manzello[1,*,†], Richard G. Gann[1], Scott R. Kukuck[2], Kuldeep Prasad[1] and Walter W. Jones[1]

[1]*Building and Fire Research Laboratory (BFRL), National Institute of Standards and Technology (NIST), Gaithersburg, MD 20899, U.S.A.*
[2]*Weapons and Materials Research Directorate, US Army Research Laboratory, APG, MD 21005, U.S.A.*

SUMMARY

A gypsum wall assembly was exposed to an intense real-scale compartment fire. For the wall assembly, temperatures were measured at the exposed face, within the stud cavity, and at the unexposed face during the fire exposure. Total heat flux gauges were used to measure the temporal variation of the energy incident on the walls, and cameras, both visual and infrared, were used to image the unexposed face of the wall assembly during the fire exposure. The behaviour of the wall assembly under the fire load is discussed as are current model results for a simulation of the fire test. Copyright © 2006 John Wiley & Sons, Ltd.

Received 28 June 2005; Revised 27 September 2006; Accepted 6 October 2006

KEY WORDS: compartmentation; fire resistance; partitions; wall; heat flux

INTRODUCTION

To mitigate fire spread in buildings, building codes dictate that compartments in buildings must be separated by fire-rated barriers or partitions. Consequently, these partitions are rated based on their resistance to the passage of heat and smoke in standard fire tests [1,2]. Use of these standards has been successful in reducing the number of fires that have killed people and destroyed structures.

Intact partitions are important in preventing the spread of flame, keeping egress paths available, and increasing safe time in places of refuge. To assess partition performance for these functions, it is necessary to know, in terms of real time, how long the interior partitions in a

*Correspondence to: Samuel L. Manzello, National Institute of Standards and Technology (NIST), 100 Bureau Drive, Stop 8662, Building 224, Room A361, Gaithersburg, MD 20889, U.S.A.
†E-mail: samuel.manzello@nist.gov
‡Official contribution of the National Institute of Standards and Technology. Not subject to copyright in the United States of America.

building will contain flames and smoke. Unfortunately, it has long been known that current fire resistance ratings obtained in furnaces do not coincide with actual safety times, but rather only provide relative guidance as to partition performance. Both the absolute response and the difference among ratings depend on the nature of the fire and the composition of a particular partition [3–6].

This suggests a high benefit to public safety of placing the fire resistance of partitions on an absolute basis. Such an advance would empower the use of prescriptive requirements while contributing to the emerging discipline of performance-based design. The Fire Research Division at NIST has embarked on a course to provide a methodology to be used in performance-based design of buildings. The research involves obtaining real-scale experimental data, modelling the behaviour of partitions as they are driven to failure by the fire, and developing recommendations for obtaining input parameters of modifications to standard fire resistance tests such as ASTM E119 [1] and ISO 834 [2]. Real-fire performance data of different types of gypsum wall constructions have been presented elsewhere [7]. To this end, a real-scale compartment test has been conducted to provide information on the phenomenology of a typical partition's response and (possible) failure under actual fire conditions. Quantitative information has also been obtained from this test to guide model development. The results of this test and model simulations are presented here.

EXPERIMENTAL DESCRIPTION

Wall assembly construction

A non-load-bearing wall consisting of gypsum panels attached to steel studs was constructed for fire testing. This construction was utilized as it is the most common interior construction for tall buildings. The 2.44 m × 2.44 m wall was constructed following ASTM guidelines for non-load-bearing wall assemblies [8–11]. The exposed face construction of the assembly is shown schematically in Figure 1. Steel studs (depth: 92 mm; width: 28.5 mm) were spaced at 609 mm and type X gypsum panels (USG Fire Code Core[§]) with a thickness of 15.9 mm were attached vertically to the studs using type S drywall screws spaced at 305 mm. The joints were taped and spackled prior to fire initiation within the compartment. As illustrated in Figure 2(a) and (b), the assembly consisted of two single (1.22 m × 2.44 m) gypsum panels installed on the exposed face and one (1.22 m × 2.44 m) gypsum panel installed on the unexposed face. Since only one side of the assembly was fitted with a gypsum panel on the unexposed face, the service holes in the studs were sealed to prevent direct exposure of the stud cavities to ambient conditions.

Test measurements

Temperature measurements were obtained using type K thermocouples (22 gauge) attached to the gypsum panels. Measurements were obtained at: (1) the exposed surface; (2) within the gypsum board cavity between the exposed and unexposed layers; and (3) on the unexposed face. Bare thermocouples were used both on the exposed face and within the gypsum board cavity. Thermocouples at the unexposed face were placed under insulating pads, as specified in ASTM E119 [1]. This was done in order to compare these measurements to the failure modes of ASTM E119 [1].

[§] Certain commercial products are identified to adequately describe the experimental procedure. This in no way implies endorsement from NIST.

DOI: 10.1002/fam

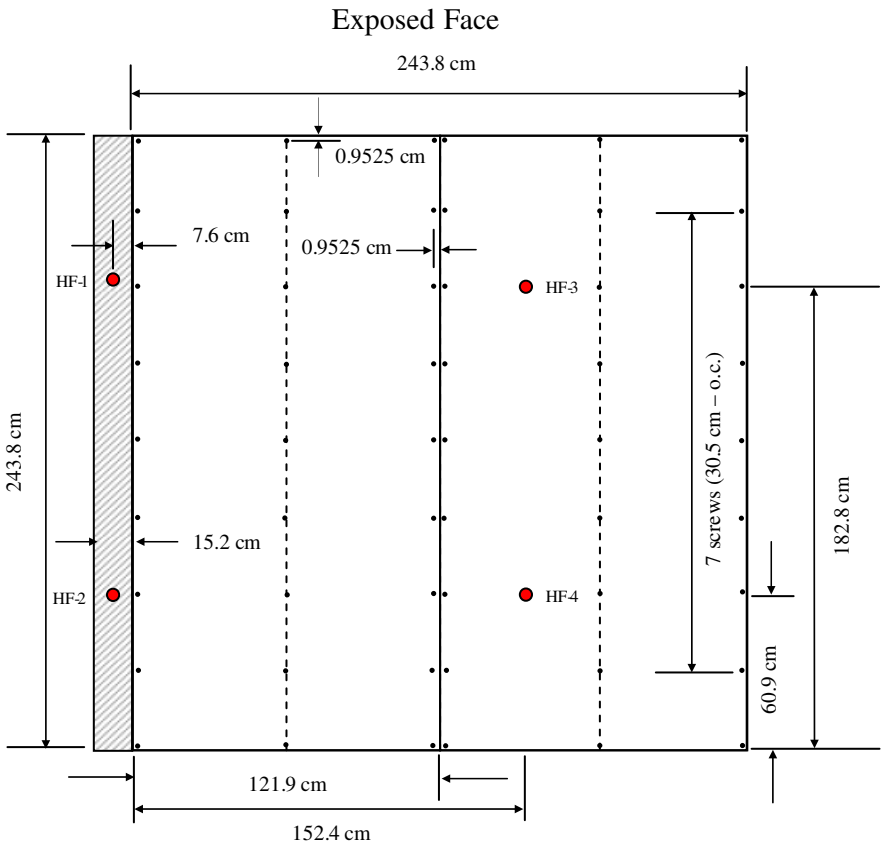

Figure 1. Drawing of partition construction at the exposed face. The location of the total heat flux gauges (HF) are shown.

Four water-cooled Schmidt–Boelter total heat flux gauges (15 mm diameter) were used to measure the heat flux incident on the walls, see Figure 1. Two gauges were mounted flush to one of the gypsum panels and two gauges were mounted flush to a column adjacent to the other vertically mounted gypsum panel. The gauges were maintained at 75°C to avoid water condensation on the surface of the gauge.

Imaging of the unexposed face of each partition assembly during testing was conducted at 30 frames/s using both a standard (visual) video camera and an infrared video camera. Both infrared and standard video cameras were recorded on mini-digital video (mini-DV) cassettes for subsequent image analysis. Photographs were taken at 2048 × 1024 pixel resolution of both the exposed and unexposed face before and after the test.

Compartment design and fire loading

The wall assembly was placed in an opening in the wall of a 10.7 m long by 7.0 m wide by 3.4 m high test compartment (Figure 3). The compartment, containing three workstations, was constructed to simulate a typical office space that would be found in tall buildings.

DOI: 10.1002/fam

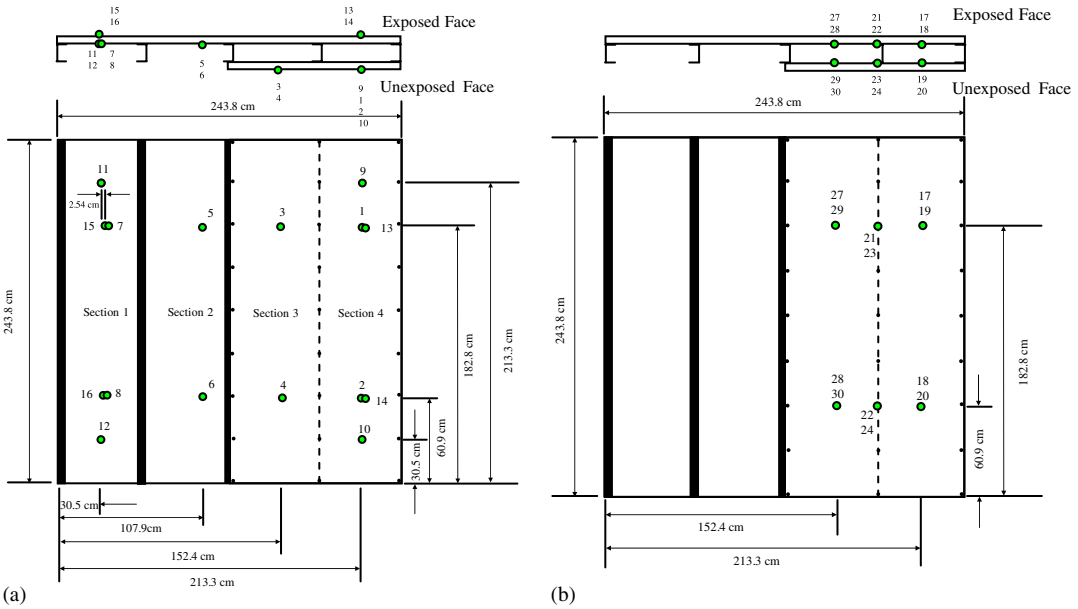

Figure 2. Drawing of the wall assembly showing the location of: (a) the unexposed face and exposed face temperature measurements; and (b) the interior temperature measurements.

The test fires were ignited using a spray burner (see Figure 3). The wall assembly was subsequently exposed to a fire with peak heat release rate (HRR) of approximately 14.0 MW, for total burn time of approximately 45 min. Further details of the combustibles and the design of the compartment are available elsewhere [12].

EXPERIMENTAL RESULTS

A picture of the exposed face of the assembly after the fire exposure, in Figure 4, shows that the wall remained in place throughout the test. Total heat flux data collected during the fire exposure are displayed in Figure 5(b). The combined uncertainty in the total heat flux measurements is estimated to be $\pm$ 10%. At location HF-1, the total heat flux increased rapidly to a peak value of 190 kW/m^2 at a time of 800 s from initiation. At this location, total heat flux was at more than 150 kW/m^2 for over 500 s. At the other upper position, HF-3, the total heat flux was 30% less. The total heat flux was similar in magnitude (130 kW/m^2) for the two lower positions, HF-2 and HF-4.

The exposed face temperature measurements for the assembly are displayed in Figure 5(a). The thermocouples located at positions 13 and 14 failed at 850 and 1150 s, respectively, into the fire exposure. Complete temperature traces were obtained at thermocouple locations 15 and 16. In spite of the thermocouple failures, significant data were obtained to provide a picture of the temperature rise on the exposed surface. From the figure, the largest temperature rise occurred at location 13, followed by thermocouple location 14.

Figure 6(a) displays interior temperature measurements on the inside of the exposed board of the double panel sections. Figure 6(b) shows interior temperatures measurements on the inside

DOI: 10.1002/fam

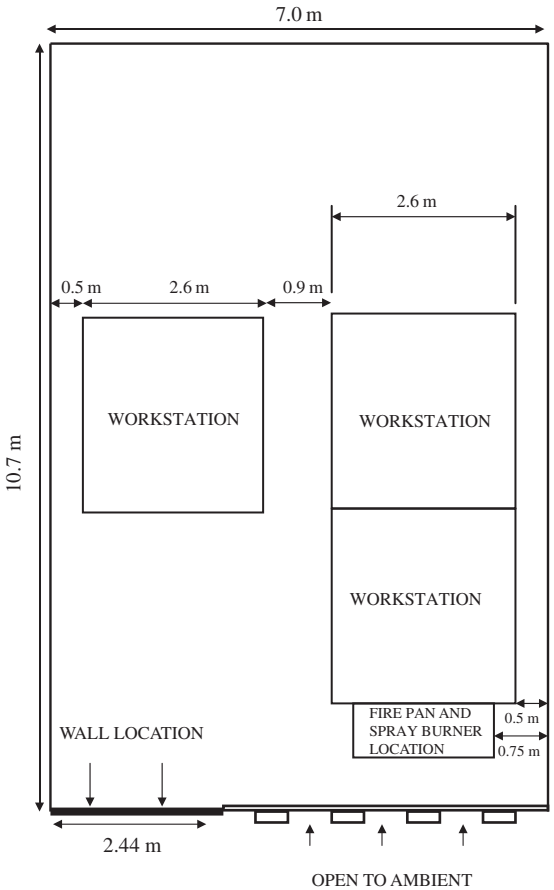

Figure 3. Schematic of compartment where the wall assembly was installed. WS—workstation.

of the unexposed board. As expected, the temperature rose faster on the inside of the exposed board at all locations compared to those temperatures at the same height on the inside of the unexposed board. A noticeable temperature increase, for example, was observed 30 s after ignition on the interior of the exposed board while, on the contrary, a temperature rise was not detected on the inside of the unexposed board until 125 s after ignition. The temperatures measured on the inside of the unexposed board also exhibited greater variation than those measured on the exposed board. For example, at location 19 the measured maximum temperature was 460°C, whereas at location 20 the measured maximum temperature was 300°C. In contrast, the variation on the interior of the exposed board was from a measured maximum temperature of 500°C at location 17 to a measured maximum of 460°C at location 22.

The outside face temperatures of the unexposed board are displayed in Figure 7. It is apparent that the temperature rise on the outside face of the unexposed board, for the double board construction, was minimal and was, in fact, insufficient to result in failure under the insulation criterion of either ASTM E119 [1] or ISO 834 [2].

DOI: 10.1002/fam

Figure 4. Digital pictures of the exposed face immediately after the fire exposure for the assembly.

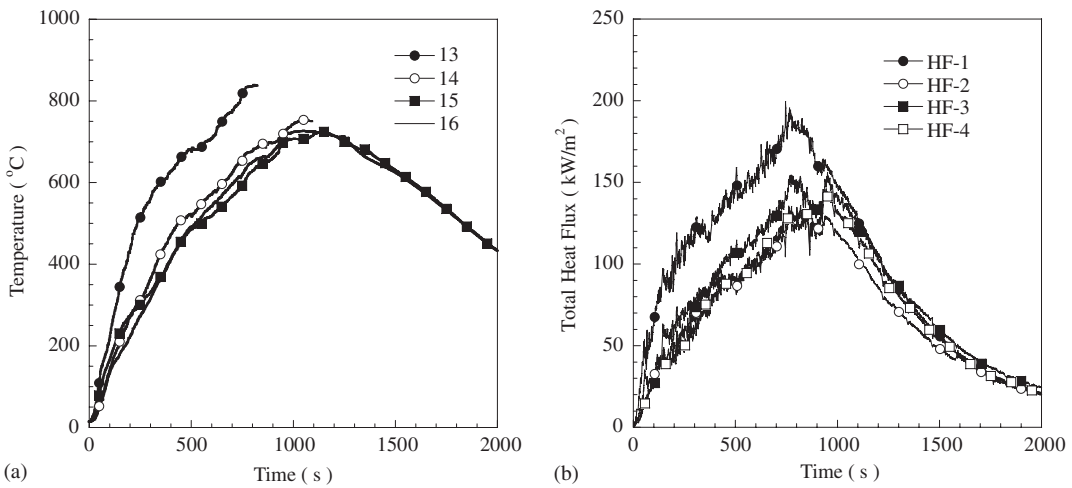

Figure 5. (a) Temporal evolution of the exposed face temperature measurements for the assembly as a function of location; and (b) temporal evolution of the total heat flux measurements for the assembly as a function of location.

DOI: 10.1002/fam

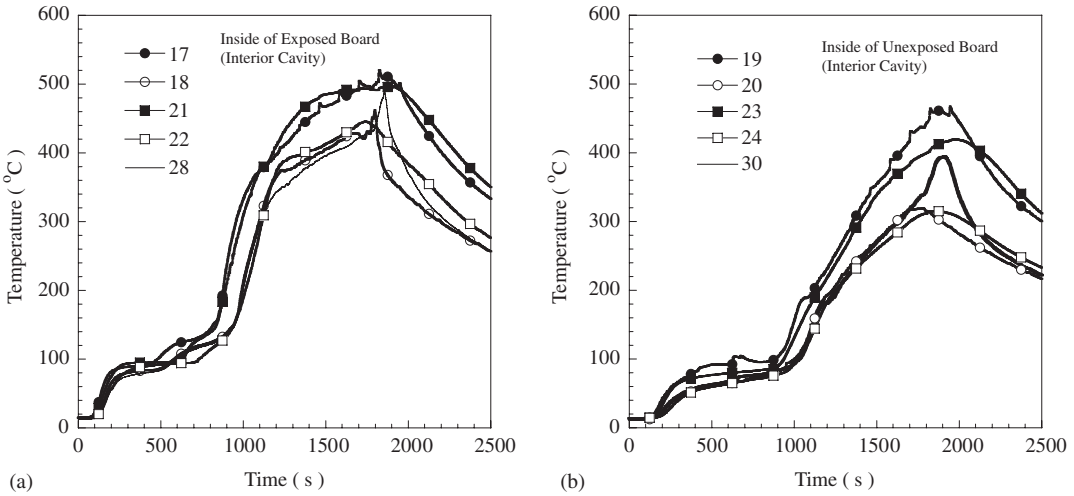

Figure 6. (a) Temporal evolution of temperatures measured on the inside of the exposed face as a function of location; and (b) temporal evolution of temperatures measured on the inside of the unexposed face as a function of location.

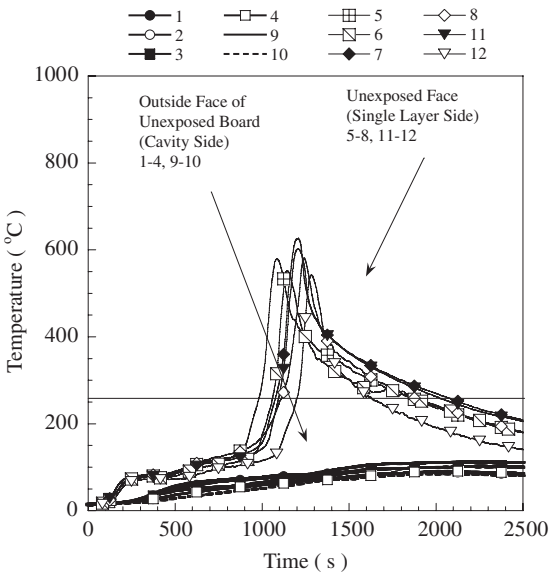

Figure 7. Measured unexposed face temperatures as a function of time and location.

For the side of the wall with only a single gypsum board, the temperature rise on the outside face was significant. The insulation failure criterion was reached at 900 s after ignition. The uncertainty in these measurements is estimated to be $\pm 10^{\circ}$C. The spatial variation in the

DOI: 10.1002/fam

temperature rise has been described in detail elsewhere, as the performance of this assembly has been compared to gypsum wall assemblies of different construction under a fire load [7].

For the single gypsum panel (on the right—see Figure 4), vertical cracks (at the screw locations) and transverse cracks were clearly visible. The transverse cracks appeared first in section 2 (t= 1494 s) and later in section 1 (t= 1708 s). For the gypsum panel on the left, part of the double panel constructions, large gaps occurred at the screw locations but transverse cracks did not appear. The unexposed face on this side was visibly unaffected by the fire exposure. As a result, the cracking that resulted on the exposed panel on this side was not visible in either the IR or standard video view.

MODEL DESCRIPTION AND RESULTS

In short, the model solves a system of partial differential equations describing the transport of heat and mass through porous, hydrated materials. The primary component of gypsum wallboard is calcium sulphate dihydrate ($CaSO_4 \cdot 2H_2O$), which has two water molecules chemically bound within the crystal for each calcium sulphate molecule. It is the water molecules, and the energy required to release them from the crystal, which gives gypsum board its fire-resistant properties. The dehydration of the calcium sulphate dehydrate typically occurs through two reversible steps [13] that occur at temperatures between 125 and 225°C:

$$CaSO_4 \cdot 2H_2O + Q \rightleftharpoons CaSO_4 \cdot \tfrac{1}{2}\,H_2O + \tfrac{3}{2}\,H_2O \tag{1}$$

$$CaSO_4 \cdot \tfrac{1}{2}\,H_2O + Q \rightleftharpoons CaSO_4 + \tfrac{1}{2}\,H_2O \tag{2}$$

At even higher, approximately 350°C, a third reaction irreversibly reorganizes the crystalline structure of the calcium sulphate to a lower, insoluble energy state.

In contrast to other models [14–16], which solve only an energy conservation equation and approximate the heat required to liberate the water molecules over fixed temperature ranges, the model used here allows for mass transport and introduces kinetic mechanisms to describe the dehydration mechanisms. While previous models have proved useful in describing the results of standard fire tests [17], the predictive capabilities for general fire exposures have shown mixed results. The model used here is an attempt to incorporate additional phenomena and, therefore, test underlying assumptions and asses gaps that may still exist in modelling partition response. Establishing the validity of these assumptions and determining conditions under which accurate results can be obtained is crucial in developing any model that will be potentially used in performance-based analyses. The current implementation of the model solves for one-dimensional, time-varying exposures.

The governing equations used in the model consist of gas-phase conservation equations, liquid-phase conservation equations, momentum conservation (i.e. Darcy's law for transport through a porous material), and the energy conservation equation. These equations are

$$\frac{\partial}{\partial t}\{\varphi_g C_1\} + \nabla \cdot \{f_g C_1 \mathbf{V}_g\} = \nabla \cdot \left\{ f_g C D \nabla \frac{C_1}{C} \right\} \tag{3}$$

DOI: 10.1002/fam

$$\frac{\partial}{\partial t}\{\varphi_g C_2\} + \nabla \cdot \{f_g C_2 \mathbf{V}_g\} = \nabla \cdot \left\{ f_g C D \nabla \frac{C_2}{C} \right\} - \frac{1}{M_2} \frac{\partial}{\partial t}\{S + W + A\} \tag{4}$$

$$\frac{\partial}{\partial t}\{\varphi_\ell \rho_\ell\} + \nabla \cdot \{f_\ell \rho_\ell \mathbf{V}_\ell\} = \frac{\partial W}{\partial t} \tag{5}$$

$$\mathbf{V} = -\frac{K}{\mu} \nabla p \tag{6}$$

$$\{SC_S + WC_\ell + AC_A\}\frac{\partial T}{\partial t} + f_\ell \rho_\ell C_\ell \mathbf{V}_\ell \cdot \nabla T = \nabla \cdot \{k_c \nabla T\} - \left\{ \Delta h_s \frac{\partial S}{\partial t} + \Delta h_\ell \frac{\partial W}{\partial t} \Delta h_A \frac{\partial A}{\partial t} \right\} \tag{7}$$

Here, φ is the pore space and f is the fraction of pore space occupied by the gas phase (subscript g) or liquid phase (subscript ℓ). C_1 is the molar concentration of gas, in the absence of water vapour, and C_2 the molar concentration of water vapour (having molecular weight M_2), with the total molar concentration given as $C = C_1 + C_2$. The convective velocity of the liquid and gas phases is denoted by $\mathbf{V}$ and is driven by pressure p. The density of the solid phase is presented above as S, the amount of condensed water as W and the amount of adsorbed water as A, with liquid water density ρ_ℓ. The temperature of all species within a representative volume is T. Mass transport parameters are the unsaturated diffusivity of water vapour D, the permeability of the gypsum board K and the viscosity of the gas phase μ. Heat transport parameters are the composite thermal conductivity k_c, specific heat of the underlying solid C_S, specific heat of condensed water C_ℓ and specific heat of adsorbed water C_A. The energies required to change state/phase are Δh_s, Δh_ℓ and Δh_A for dehydration/hydration, evaporation/condensation and adsorption/desorption, respectively.

For the internal air wall cavity, i.e. stud spaces, the model uses a lumped approach, assuming a well-mixed control volume. Sufficient leakage points are assumed to exist that maintain a constant pressure. Governing equations conserve gas species:

$$V \frac{\partial C_1}{\partial t} = \oint_A C_1'' \, \mathrm{d}A - V \dot{C}_{1e} \tag{8}$$

$$V \frac{\partial C_2}{\partial t} = \oint_A C_2'' \, \mathrm{d}A - V \dot{C}_{2e} \tag{9}$$

and energy

$$V \frac{\partial}{\partial t}\{C_1 u_1 + C_2 u_2\} = \oint_A \{C_1'' h_1 + C_1'' h_1 + q''\} \, \mathrm{d}A - V\{\dot{C}_{1e} h_{1e} + \dot{C}_{1e} h_{1e}\} \tag{10}$$

where V is the volume of the gas layer and A is the associate area of the boundaries. Terms with the subscript e represent flows that must exist so as to satisfy the constant pressure constraint.

For both the gypsum board and internal stud spaces, the governing equations are supplemented by appropriate equations of state. The gas phases are considered ideal,

DOI: 10.1002/fam

multicomponent mixtures:

$$p_1 = C_1 RT \tag{11}$$

$$p_2 = C_2 RT \tag{12}$$

with

$$p = p_1 + p_2 \tag{13}$$

The liquid phase is considered incompressible with condensation/evaporation governed by the local partial pressure of the water vapour as a function of temperature only, i.e. $p_{sat} = p_{sat}(T)$.

The numerical solution is nominally second order in space and first order in time. Diffusive quantities are evaluated using second-order central differences with convective terms evaluated using upwind biasing. The temporal scheme uses a backward Euler approach, so as to reduce stability issues.

For the simulation discussed here, we note from Figure 5(b) that with the exception of the heat flux measured at location 1 (upper column) the other heat fluxes were similar in nature. While the upper flux away from the column was greater than those measured on the lower portion of the wall, it is still of the same order of magnitude. We have chosen, therefore, to average the measured heat flux from gauges HF-2, HF-3, and HF-4 and use the result as the thermal insult to the simulated wall.

Two simulations were conducted, one for each half of the wall assembly. The results for a single exposed gypsum board are displayed in Figure 8, while the results for one gypsum board on either side of a stud cavity are displayed in Figure 9. The experimental results shown in the figures have been calculated, in similar manner as earlier, as averages of the thermocouples at various depths through the assembly. As earlier, we have neglected those thermocouple measurements located closest to the upper column heat flux gauge. Thus, for example, the exposed face measurement is the arithmetic average of thermocouples 14–16. Error bars denote the upper and lower maximum deviations from the average, thus representing the spread of the measured results.

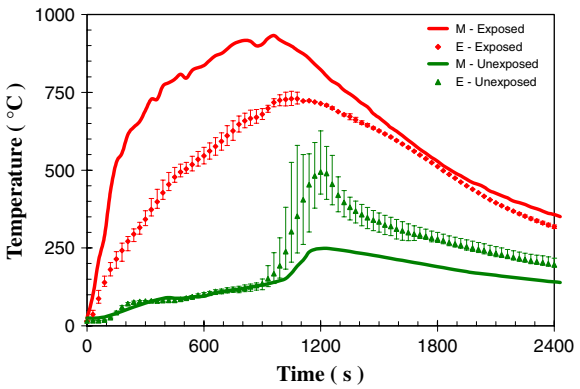

Figure 8. Comparison of model results (curves) with experimental measurements (points) for the single gypsum board exposure. The error bars denote the spread of the measured results about the calculated average.

DOI: 10.1002/fam

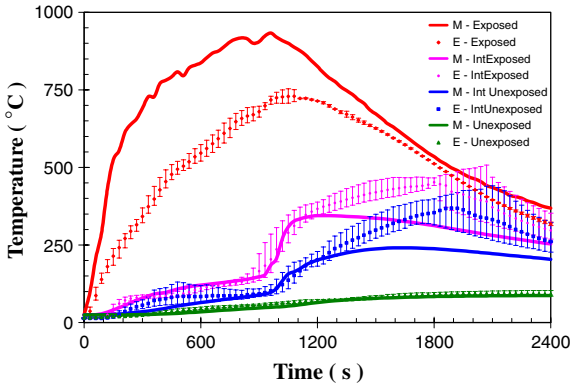

Figure 9. Comparison of model results (curves) with experimental measurements (points) for the gypsum board/stud cavity exposure. The error bars denote the spread of the measured results about the calculated average.

Exposed face temperatures, determined from the simulation, are over-predicted compared to experimental measurements. Of all the reported results, these have the largest uncertainty due to the inherent difficulty of measuring surface temperatures within the fire environment. It has been shown that differences of greater than 100°C, for exposed surfaces of insulating materials, may be realized [18]. These differences were attributed to the low thermal mass and high conductivity of the thermocouples. An additional complication for these measurements is the potential cooling of imbedded wires from the dehydration reactions in the gypsum board. This effect would act to reduce the measured temperatures.

For the single board simulation, we see that the model accurately predicts the temperature of the unexposed face for approximately the first 1000 s of the test. From this point, the results of the model and experiment diverge significantly. Even with this divergence, the model prediction for insulation failure at 1065 s compares reasonably with the experimental average at 965 s.

Three possible explanations for the deviations between the model and experiment may be considered. The first two relate to the phenomenological response of the gypsum board that is not captured by the model. First, gaps began to develop at the seams and centre studs at approximately 1000 and 1300 s, respectively. These gaps allowed hot gases to begin to penetrate the board, increasing the heat transfer at these locations. The second response not accounted for by the model is the ignition and burning of the paper backing, which would also result in an increased temperature response. The third possible explanation is that the model does not include the effect of the pad placed over the thermocouples on the unexposed face. The current simulation has neglected to include the effect that the pad would have on the measured temperature. As the model is developed further, it will become necessary to incorporate these effects [19].

For the simulation of the gypsum boards installed on either side of a stud cavity, similar qualitative comparisons are observed. For the interior temperature measurements, the model again accurately simulates the response for approximately the first 1200 s of the test. Beyond this point, as the peak heat flux has been reached and the fire exposure was fading, the model predicts the temperatures to level and then decay. In contrast, the experimental results showed that the temperature for the interior surfaces continued to increase until about 2000 s into the test. This behaviour may be attributed to gap formation at the seams and center studs that

DOI: 10.1002/fam

are not accounted for in the model. The model does, however, accurately predict the temperature of the unexposed surface of the board for the full range of results presented.

DISCUSSION

This work bears on the evolution of an advanced paradigm for compartmentation durability in fires in three ways. To be of such value, a partition should withstand the transport of heat, smoke and toxic gases, and flames.

The first contribution addresses the differences between the standard furnace conditions and the fire. Sultan *et al*. [20] had shown that in a large-scale, ASTM E119 [1]-like furnace designed to test walls and floors, the total heat flux measured was nearly identical (within 2%) at the two gauge locations. In the current fire test, there is a 30% variation in heat flux and a 200°C variation over the surface of the wall assembly. This is the result of testing under real-fire conditions and not in a furnace. In addition, the rate of increase of total heat flux measured in the furnace was slower than measurements in the present fire environments. In Figure 5(b), the total heat flux reached 100 kW/m^2 in 700 s. In the furnace, this did not occur until 40 min (2400 s) [20]. At present, it is not known how important these gradients are in effecting partition failure faster than in a uniform field.

The second is a comparison of the rates of temperature rise in this fire test and those of Sultan [19] in test of similar walls in a furnace. The most dramatic difference between the measurements of Sultan [19] and those of present assembly is the rate of temperature rise, both inside the cavity and on the outside face of unexposed board. For example, the time to reach an average temperature of 350°C on the inside of the exposed board of the double panel sections was 1100 s, as compared to 1550 s in the furnace test [19].

The third is the contribution of the current computational model for predicting wall failure. The results simulating the single exposed gypsum board and the wall section with one gypsum board on either side of a stud cavity showed good agreement with the experimental measurements for approximately the first 1000–1200 s. Beyond these times, the model under-predicted the temperatures. Physically reasonable features of the partition's fire response (gypsum board contraction and gypsum board cracking) are now being incorporated into the model. The model of Takeda [21] has begun to address some of this by incorporating the contraction of gypsum board on the exposed face at the seams in his model.

However, the standard temperature criterion is itself of marginal value in assessing fire hazard. Autoignition of combustibles on the unexposed side of the wall requires both much higher temperatures and good thermal contact between the wall and the combustibles. Moreover, for a performance-based design approach, it is important to know when the wall partition assemblies collapse and when their effectiveness as a smoke and flame barrier is compromised due to gypsum board shrinkage and cracking. This and any other model needs to be extended to predict the loss of partition integrity that leads to the passage of heat and smoke.

CONCLUSIONS

A wall assembly of 2.44 m × 2.44 m was exposed to an intense fire from the time of ignition to beyond flashover. During the fire exposure, temperatures were measured at the exposed surface,

DOI: 10.1002/fam

within the gypsum board cavity, and at the unexposed face. Total heat flux gauges were used to measure the time histories of the energy incident on the walls, and visual and infrared cameras were used to image the unexposed face during fire testing. For the side of the wall utilizing a gypsum board on either side of a stud cavity, the partition did not experience an insulation failure based upon current rating systems [1,2]. In the actual fire, as opposed to a furnace test, the total heat flux was clearly a function of location. In addition, the rate of increase of total heat flux measured in the fire was considerably faster than that observed in furnace tests.

Model results simulating both the single board and the gypsum on either side of a stud cavity showed good agreement with experimental measurements for approximately the first 1000–1200 s. Beyond these points, the model under-predicted the temperature. Among possible explanations currently being explored are phenomenological responses not incorporated into the model, such as gap formation and burning of the paper backing, as well as the influence of the insulting pad, required under ASTM E119 [1], on the veracity of the surface temperature measurements.

ACKNOWLEDGEMENTS

The authors acknowledge the staff of the Large Fire Laboratory (Mr Alexander Maranghides, Mr Jay McElroy, Mr Lauren DeLauter, Mr Ed Hnetkovsky, and Mr Jack Lee) for assistance in the experiments.

REFERENCES

1. American Society for Testing and Materials. *Test Method for Fire Resistance Tests of Building Construction and Materials*. ASTM E119-00a.
2. International Organization for Standardization. *Fire Resistance Tests—Elements of Building Construction*, *ISO 834*. Parts 1–9. International Organization for Standardization: Geneva, Switzerland.
3. Bukowski RW. Prediction of the structural fire performance of buildings. *Eighth Fire and Materials Conference*, San Francisco, CA, 2003.
4. Keltner NR, Moya JL. Defining the thermal environment in fire tests. *Fire and Materials* 1989; **14**:133–138.
5. Grosshandler WL (ed.). *Fire Resistance Determination and Performance Prediction Research Needs Workshop*: *Proceedings*, NISTIR 6890, 2002.
6. CIB-W14. Rational Fire Safety Engineering Approach to Fire Resistance of Buildings, Publication 269, 2001.
7. Manzello SL, Gann RG, Kukuck SR, Prasad K, Jones WW. Real fire performance of partition assemblies. *Fire and Materials* 2005; **29**:351–366.
8. American Society for Testing and Materials. *Standard Specification for Installation of Steel Framing Members to Receive Screw-Attached Gypsum Panel Products*. ASTM C754-00.
9. American Society for Testing and Materials. *Standard Specification for Application of Finishing of Gypsum Board*. ASTM C840-03.
10. American Society for Testing and Materials. *Standard Specification for Nonstructural Steel Framing Members*. ASTM C654-00.
11. American Society for Testing and Materials. *Standard Specification for Steel-Piercing Tapping Screws for the Application of Gypsum Panel Products or Metal Plaster Bases to Wood or Steel Studs*. ASTM C1002-01.
12. Hamins A, Maranghides A, McGrattan K, Ohlemiller T, Anleitner R. Federal building and fire safety investigation of the world trade center disaster: experiments and modeling of the multiple workstations burning in a compartment. *NIST NCSTAR 1-5E*, 2005.
13. Ramachandran VS, Paroli RM, Beaudoin JJ, Delgado AH. *Handbook of Thermal Analysis of Construction Materials*. Noyes Publications: Norwich, NY, 2003.
14. Thomas G. Thermal properties of gypsum plasterboard at high temperatures. *Fire and Materials* 2002; **26**:37–45.
15. Mehaffey JR, Cuerrier P, Carisse GA. A model for predicting heat transfer through gypsum-board/wood-stud walls exposed to fire. *Fire and Materials* 1994; **18**:297–305.
16. Collier PCR, Buchanan AH. Fire resistance of lightweight timber framed walls. *Fire Technology* 2002; **38**:125–145.

DOI: 10.1002/fam

17. Hurst JP, Ahmed GN. Modeling the thermal response of gypsum wallboard and stud assemblies subjected to standard fire testing. *International Conference on Fire Research and Engineering—Proceedings*, Orlando, FL, 1995.
18. Hamins A, Maranghides A, McGrattan K, Ohlemiller T, Yang J, Donnelly M, Mulholland G, Prasad K, Kukuck S, McAllister T. Experiments and thermal modeling of structural steel elements exposed to a fire. *NIST Special Publication 1000-10B*, 2005.
19. Sultan MA. A model for predicting heat transfer through noninsulated unloaded steel-stud gypsum board wall assemblies exposed to fire. *Fire Technology* 1996; **32**:239–259.
20. Sultan MA, Benichou N, Min BY. Heat exposure in fire resistance furnaces: full-scale *vs* intermediate-scale. *Eighth Fire and Materials Conference*, San Francisco, CA, 2003.
21. Takeda H. A model to predict the fire resistance of non-load bearing wood-stud walls. *Fire and Materials* 2003; **27**:19–39.

DOI: 10.1002/fam